

# A Refined Quasi-Static Method for Precise Determination of Piezoelectric Coefficient of Nanostructured Standard and Inclined Thin Films

Manuel Pelayo Garcia, Desmond Gibson, Dave Allan Hughes, and Carlos Garcia Nuñez\*

Piezoelectric materials are key components for applications including non-destructive testing, medical imaging, energy harvesting, ultrasonic sensors, and actuators. Among different materials exhibiting piezoelectricity, crystalline thin films are proposed as alternative candidates to replace ceramics due to their high integrability in micro-/nano-scale devices and compatibility with non-conventional flexible/wearable substrates. To measure the piezoelectric response, Berlincourt (BC) quasi-static method is proposed as one of the simplest, however for thin films this method has not yet been explored in sufficient detail. This paper reports the effects of measuring BC parameters on the resulting piezoelectric coefficient ( $d_{33}$ ) of sputter deposited ZnO with the shape of standard and inclined nanostructured thin films. Results provide comprehensive, reliable and repeatable information about true piezoelectric coefficient of thin films ( $6.0 \pm 0.1 \text{ pC N}^{-1}$  for standard;  $24 \pm 1 \text{ pC N}^{-1}$  for inclined films) by selecting optimized parameters in BC measurements, including dynamic force ( $0.45 \text{ N}_{pp}$ ), static force (1 N) and frequency (110 Hz), utilizing the protocol here named Method 2 for clamping the film, and measuring after the stage of high variability has passed ( $t > 1200 \text{ s}$ ). Additionally, this modified BC has allowed the indirect estimation of stress accumulated in the ZnO lattice during measurements, offering a reliable and repeatable method for the determination of true  $d_{33}$  in crystalline thin films.

## 1. Introduction

Piezoelectric materials play a crucial role in sensors<sup>[1,2]</sup> and actuators<sup>[3]</sup> used in a wide range of applications, including medical imaging, non-destructive testing (NDT), and infrastructure monitoring.<sup>[4-6]</sup> Among all properties, the piezoelectric coefficient ( $d_{33}$ ) serves as a fundamental measure of piezoelectric materials capacity to generate an electric charge flow that aligns with the direction of an applied external mechanical stimulus. This coefficient depends mainly on material properties (crystal structure, crystal symmetry, morphology, and composition), and characterization parameters (temperature, frequency and amplitude of an externally applied mechanical and electrical stimuli).<sup>[7]</sup> In addition, the doping (type and level) and fabrication method utilized to synthesize a piezoelectric material, have been demonstrated to influence the resulting atomic structure of the piezoelectric material, causing drastic changes in the  $d_{33}$  coefficient.<sup>[8]</sup> As such, this makes

the investigation of new and more accurate metrology methods to measure the true value of  $d_{33}$  coefficient an essential aspect to tailor and optimize the material to the required performance, depending on the application.<sup>[1-6]</sup>


Commonly, ceramics such as lead magnesium niobate-lead titanate (PMN-PT), strontium titanate ( $\text{SrTiO}_3$ ) or lead zirconate titanate (PZT) are used in aforementioned applications due to their high piezoelectric coefficients (e.g., PZT presents a  $d_{33}$  ranged from 100 to 500  $\text{pC N}^{-1}$ ).<sup>[9]</sup> However, concerns have been highlighted about the environmental impact and toxicity of these materials due to their lead content.<sup>[10,11]</sup> Therefore, it is critical and timely to investigate alternative material choices in support of the global effort to provide environmentally friendly piezoelectric materials. In this regard, crystalline piezoelectric materials with the shape of thin films and based on earth-abundant elements such as oxygen and nitrogen (e.g., zinc oxide, ZnO; aluminum nitride, AlN; or gallium nitride, GaN) are recent candidates as potential lead-free eco-friendly alternatives for future sensing/actuating applications.<sup>[12]</sup> Even though their piezoelectric coefficients are not comparable to ceramics ( $d_{33, \text{ZnO}} = 10\text{--}15 \text{ pC N}^{-1}$ ;  $d_{33, \text{AlN}} = 5\text{--}10 \text{ pC N}^{-1}$ ; and  $d_{33, \text{GaN}} = 1\text{--}5 \text{ pC N}^{-1}$ )<sup>[13]</sup> they offer

M. P. Garcia, D. Gibson, C. G. Nuñez  
Institute of Thin Films, Sensors and Imaging  
University of the West of Scotland  
Paisley PA1 2BE, UK  
E-mail: carlos.garcianunez@glasgow.ac.uk

D. Gibson  
AlbaSense Ltd  
Paisley PA1 2BE, UK

D. A. Hughes  
Novosound Ltd  
Motherwell ML1 5UH, UK

C. G. Nuñez  
University of Glasgow  
Glasgow G12 8QQ, UK

 The ORCID identification number(s) for the author(s) of this article can be found under <https://doi.org/10.1002/apxr.202300091>

© 2023 The Authors. Advanced Physics Research published by Wiley-VCH GmbH. This is an open access article under the terms of the Creative Commons Attribution License, which permits use, distribution and reproduction in any medium, provided the original work is properly cited.

DOI: 10.1002/apxr.202300091

several advantages. They can be miniaturized and integrated in other micro- and nano-electronic components, allowing the fabrication of mass producible low-cost compact, highly integrated and multifunctional devices (e.g., nano-generators or micro-manipulators).<sup>[14–16]</sup> Also, they can be easily deposited by physical vapor deposition (PVD) techniques in a controlled manner and on a wide range of substrates, including flexible substrates (e.g., polyethylene terephthalate, PET; polyimide, PI; metallic foils), allowing precise control of thickness, composition, and industrial scalability for high-volume low-cost production.

The low value of  $d_{33}$  in these thin film materials has initiated an intensive number of investigations of new and more accurate experimental setups to precisely measure material  $d_{33}$  coefficient. As such, a number of techniques, including: laser interferometers, laser scanning vibrometers, piezoelectric force microscopes, and direct measurements of the stress-induced charge (Berlincourt method) have been reported in the literature describing a potential way to measure both direct and indirect piezoelectric coefficient.

Laser doppler vibrometry (LDV)<sup>[17,18]</sup> and piezoelectric force microscopy (PFM),<sup>[19,20]</sup> have been utilized for the measurement of indirect piezoelectric effect in both bulk and thin piezoelectric films. As briefly summarized below, LDV and PFM techniques present great advantages for the characterization of piezoelectric thin films over Berlincourt (BC), but also show critical drawbacks encouraging scientific community to keep exploring for alternative methods.

LDV consists of an interferometric technique where a laser beam is directed to the surface of the piezoelectric material which would be electrically excited at a certain frequency and amplitude. The reflected laser is then compared with a reference beam and from the intensity overlap information the displacement of the sample is extracted, therefore obtaining the piezoelectric coefficient  $d_{33}$  in  $\text{pm V}^{-1}$ . This technique allows the non-contact characterization of thin film piezoelectric materials with high resolution and precision; however, it has several limitations.<sup>[17]</sup> It requires of a reflective surface for the measurement to be accurate enough, therefore compromising the characterization of complex diffusive surfaces. Also, it is challenging to account for the contribution of the substrate bending to the measured  $d_{33}$ , resulting in an overestimation of the coefficient.<sup>[18]</sup> The system also requires an accurate calibration and pre-alignment of the laser beam on the sample surface which requires software compensation and limits the use of LDV to analyze piezoelectric behaviors over time. The correction of these features increases the cost of the equipment and time for the use of LDV in thin film piezoelectric characterization.

PFM is also used to measure the indirect  $d_{33}$  coefficient in thin films. It consists of a traditional atomic force microscope (AFM) used with a conductive tip that allows the local application of an electric field across the sample under test.<sup>[19,20]</sup> This technique allows the investigation of piezoelectric/ferroelectric local domains with high resolution, producing mapping images of piezoelectric materials showing both topography and polarization of the sample.<sup>[21]</sup> The main limitations of this technique are the cost and the time per measurement, as it requires expensive equipment and high-cost electronics to achieve a stable, accurate measurement. Moreover, the PFM only focuses the analysis on micrometric window of analysis which limits drastically the lateral

resolution of the technique, and thus the evaluation of the surface uniformity in wafer scale samples.

Alternatively, Berlincourt, or also known as quasi-static method, has been commonly used to characterize the direct piezoelectric effect in bulk ceramics due to its simplicity, versatility, high sensitivity, and fast reading of the  $d_{33}$ .<sup>[9,22]</sup> However, its direct application to measure  $d_{33}$  in thin films is still unclear mainly due to the difficulty of generating a homogeneous uniaxial stress on a film deposited on a thick substrate without the substrate bending, which would overestimate the piezoelectric coefficient  $d_{33}$  due to the contribution of the transverse piezoelectric effect.<sup>[23]</sup> As a result, modifications such as a pneumatic pressure rig<sup>[24]</sup> and sample flexure techniques<sup>[25–27]</sup> have been suggested to improve this method. Despite those efforts, there is still room for improvement in the BC method, as these enhanced techniques still require of either some hardware modifications or intricate post-measurement analysis by the use of derived equations from finite element analysis (FEA) models, that consequently increases the complexity of the simple BC system.

The BC piezoelectric meter system consists of a force head unit (**Figure 1a**) and an electronics unit, the latter controlling the actuation of the head and the acquisition of the data. As illustrated in (**Figure 1a**), the sample is sandwiched between top (*ground*) and bottom (*active*) electrodes. The applied static force ( $F_s$ ), also termed clamping force, is measured by a load cell located underneath the bottom electrode (**Figure 1a**). Once the sample is clamped at the desired  $F_s$  the electronics unit is used to apply an oscillating dynamic force ( $F_d$ ) with a specific amplitude ( $F_0$ ) and frequency ( $f$ ). The deformation of the material in above conditions produce an electric charge flow that is measured by the electronics unit, displaying the resulting  $d_{33}$  coefficient in  $\text{pC N}^{-1}$ <sup>[28]</sup> (**Figure 1a**). To optimize the process, in this work, a Python algorithm has been developed (**Figure 1b**). This algorithm is designed in two logic blocks, comprising: experimental setup (yellow block in **Figure 1b**) and measure protocol (*green block* in **Figure 1b**). The interconnection between these two blocks guarantees the successful study of piezoelectric thin films. As schematically described in **Figure 1b**, once the sample is loaded into the system, the static force is adjusted until the measurement  $F_s$  is achieved. Once the developed script takes control and adjusts the dynamic force, both  $F_0$  and  $f$ , to the set values for the study. The system then starts acquiring data from three channels,  $d_{33}$ , temperature and relative humidity. If the current study requires, for example, a change in  $F_d$ , the system adjusts the value and sends command to the piezometer to sweep that parameter, accumulating all the data. When the study is finished, the data is saved together with all the experimental parameters. Then the sample can be unloaded for the next sample to be measured. This step could be also used to allow the sample to “relax” for a certain time prior to the next measurement.

That simple method has been reported to have systematic errors that contribute to a misestimation of the piezoelectric response.<sup>[14]</sup> However, comprehensive studies are available specifically for ceramics, accounting for these errors and providing information on how different parameters can affect the measurements (e.g., excitation frequency,  $F_s$ ,  $F_d$ , temperature, humidity or measurement time).<sup>[14]</sup> One of the most promising upgrades of this system is the use of a centering ring (**Figure 1c**). The role of this ring is to ensure the loading of the sample is

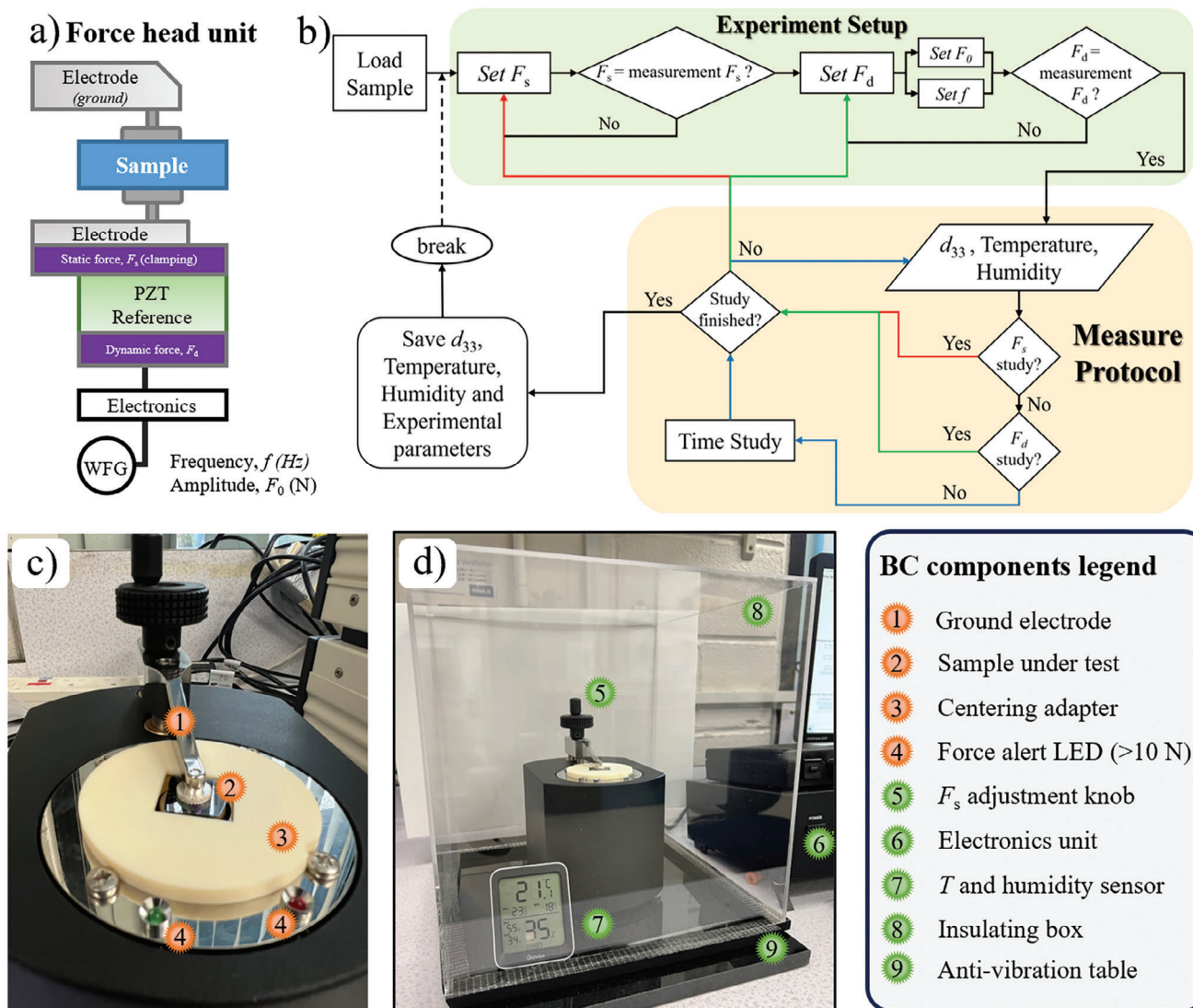


**Figure 1.** a) Schematic diagram of the force head unit. b) Logic block diagram describing the process control by Python script. c) Photograph of the BC system labelling those components used to center and clamp the sample. d) Photograph of the BC system showing the monitoring of the environmental conditions (relative humidity and temperature), as well as anti-vibration insulation.

carried out in the same way, leading to a drastic improvement in the reliability and repeatability as demonstrated later. The second improvement of a BC system is the insulation from ambient conditions including vibrations sources and environmental conditions (temperature changes, % humidity variations, pressure, gas concentration, etc.). Figure 1d shows an insulating box designed in this work to control and monitor the conditions of the measurements, and positively contribute to make the  $d_{33}$  measurements more repeatable and reliable. This feature is key for the validation of the piezoelectric thin films prior to their utilization and deployment in commercial applications. Therefore, characterization of piezoelectric thin films using BC technique is promising but is still in need of improvement for it to be used as standard, as these materials exhibit different challenges due to the nature of their structure. For that reason, similar comprehensive studies must be made to fully adapt this straightforward

technique to thin films. The optimization of this method for thin films provides a significant tool to improvement the understanding of how certain parameters affect the piezoelectric material characterization, providing an alternative to more expensive and time-consuming techniques.

In this work, we have adapted and optimized the Berlincourt method for the characterization of piezoelectric thin and nanostructured films. Specifically, we have carried out a comprehensive study of the influence of the excitation frequency, dynamic force, and clamping force on the  $d_{33}$  coefficient, as well as explored potential ferroelectric (hysteresis), temperature, and humidity effects on this coefficient. Moreover, we have analyzed how the continuous stress affects the  $d_{33}$  over time, as a function of both dynamic and clamping forces, discussing potential current discharge effects and mechanical relaxations. The work is supported by FEA modelling of the system.

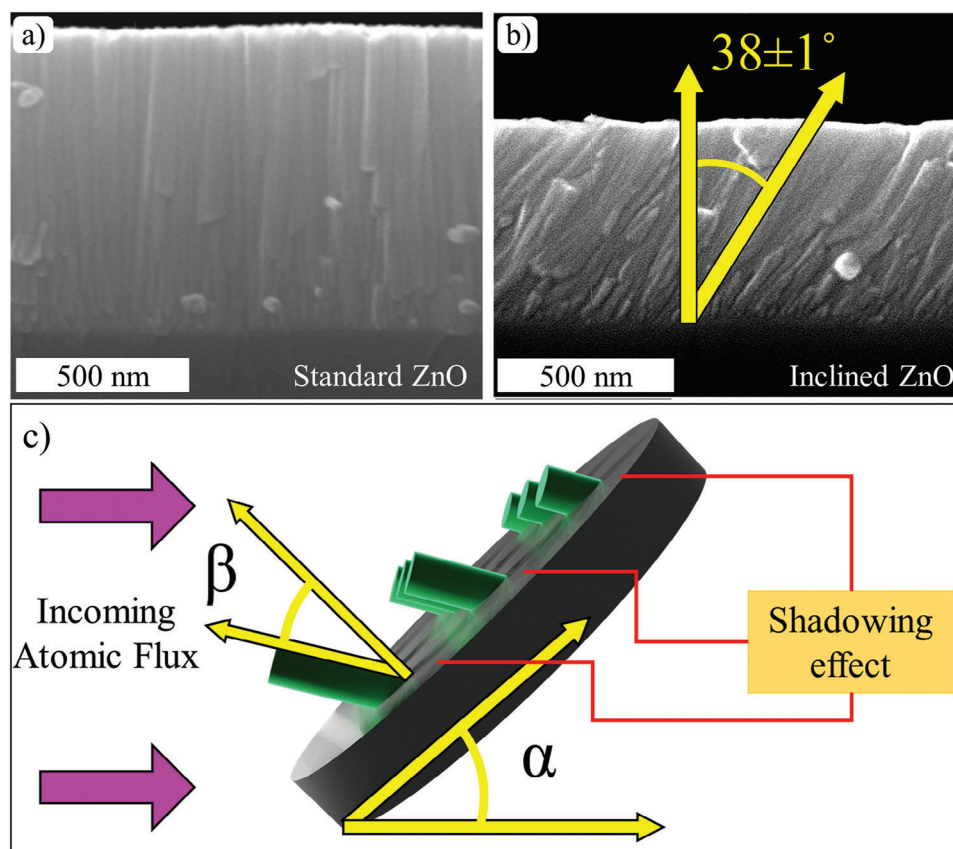


**Figure 2.** SEM images (cross-section view) of a) standard and b)  $\beta = 38 \pm 1^\circ$  inclined ZnO nanostructured thin films produced by DCRMS. c) OAD schematic representing the shadowing effect and the angles definition.  $\alpha$  represents the angle between the incoming flux and the base of the substrate.  $\beta$  represents the resulting morphological columnar inclination angle.

## 2. Experimental Section

### 2.1. Piezoelectric Characterization

The piezoelectric coefficient of thin films was characterized by using a modified BC  $d_{33}$  meter (PM-300 from Piezotest Ltd). The BC system was adapted for the measurement of thin films by mounting a 3D printed sample enclosure capable of preventing radial motion of the samples, whilst allowing its azimuthal motion (essential for  $d_{33}$  measurements). The piece made of polylactic acid (PLA) locates a 20 mm<sup>2</sup> sample centered with the  $d_{33}$  meter electrodes, the material exhibited a surface resistance in the order of the 10<sup>12</sup>  $\Omega$ , therefore expecting negligible effect on the piezoelectric measurement (Figure 1b). The use of this adaptor offered two advantages, including: i) more reliable and repeatable measurements since the samples were always mounted in the same position and the electric contact between the piezoelectric and the electrodes remains the same from measurement to measurement; ii) possibility to measure  $d_{33}$  at a wider range of clamping forces, due to the enclosure prevented the radial motion of samples. The latter opens new areas of fundamental studies that were not accessible by standard  $d_{33}$  meter conditions (typically 10 N of clamping force).

This BC system offered the possibility to measure the  $d_{33}$  coefficient under different conditions, including dynamic forces be-

tween 0.05 and 0.5 N<sub>pp</sub> with 0.05 N<sub>pp</sub> steps, static clamping forces between 0 and 10 N, with a 0.1 N accuracy, and excitation frequencies between 30 and 300 Hz with 1 Hz steps. In this work, a Python-based script was developed to program the modified BC  $d_{33}$  meter, adding new functionalities to the system, including the  $d_{33}$  measurements over time, and parameter sweeps for dynamic force (amplitude, and frequency) and static force (see Figures S1–S4 in Supporting Information). Moreover, the developed code allowed the characterization of hysteresis loops in the studied films (Figure 1c) and essential feature missing in most of the commercial systems, enabling, e.g., the analysis of ferroelectric behaviors in this kind of materials. These new features allowed the comprehensive characterization of piezoelectric effect in crystalline thin films.

### 2.2. Thin Film Deposition

Piezoelectric thin films studied in this work comprised both standard (Figure 2a) and inclined (Figure 2b) nanostructured ZnO thin films deposited on Si<sub>100</sub> substrates by direct current reactive magnetron sputtering (DCRMS), using growth parameters optimized elsewhere.<sup>[29]</sup> Inclined films were deposited by DCRMS under oblique angle deposition (OAD) conditions. As schematically described in Figure 2c, OAD consists of a tilted substrate

holder ( $\alpha$  angle) where substrates were placed, resulting in inclined thin films after deposition ( $\beta$  angle). The inclined film is generated as a consequence of the so-called “shadowing effect” occurring naturally in OAD processes (Figure 2c). More details about this technique could be found in previous research.<sup>[29]</sup>

### 2.3. Thin Film Characterization

The morphology and composition of the resulting films were characterized by scanning electron microscopy (SEM) at 20 kV and energy dispersive X-ray (EDX) analysis (Hitachi S4100 cold FEG). The tilt of the ZnO structure was determined using ImageJ software.<sup>[30]</sup> To ensure accurate calculations, the resulting angle of 20 microcolumns was measured at various sections of the sample. The final value and standard deviation were obtained by averaging these measurements. X-ray diffraction (XRD) analysis was performed to characterize the (0002) peak of the standard ZnO wurtzite structure (Siemens D5000 Cu  $K\alpha$ , 40 kV/30 mA).

Figures 2a,b shows SEM images of ZnO thin films deposited by DCMRS under standard and OAD conditions, respectively. There could be observed a difference in the column inclination angle and the total thickness of the samples. Whereas in Figure 2a the standard ZnO film shows a structure with vertical columns, i.e.,  $\beta \approx 0^\circ$ , and a thickness of  $1 \pm 0.2 \mu\text{m}$ ; Figure 2b shows for inclined ZnO an inclination angle  $\beta$  of  $38 \pm 1^\circ$  and a reduced thickness of  $750 \pm 150 \text{ nm}$  was observed. The reduction in thickness effect was explained with the reduction of the substrate-reaching atomic flux due to the physical limitation happening when the substrate is inclined. Here, standard (Figure 2a) and inclined (Figure 2b) ZnO films were used to test and validate the modified BC method not only for thin films but also for more complex morphologies such as inclined films.

### 2.4. Clamping Methodology Description

To further expand the use of BC for thin film characterization, two different measurement methods were investigated. Method 1 consisted of clamping the sample without any control over the area under investigation. The clamping area consisted of a round 2 cm diameter flat Ti electrode. Method 2, in counterpart, consisted of using the self-centering ring as reference to ensure the clamped area was exactly the same every measurement. To test the efficacy and compare both methods, the  $d_{33}$  was monitored in 10 min intervals with 10 min break for relaxation between measurement. Within the 10 min break the sample under testing was removed from the system and placed on a flat non-conductive surface, after the break the sample was clamped back into the BC following one of the respective methods.

### 2.5. Finite Element Analysis Model Description

The results were supported by FEA simulations by using the Piezoelectricity Module in COMSOL Multiphysics.<sup>[31]</sup> The model consisted of a 2 cm diameter geometry, matching the clamped area of the investigated material. The geometry is divided into a  $1 \mu\text{m}$  ZnO thin film placed on top of a 1 mm Si piece. The

electromechanical coupling of both materials was ensured by the creation of a contact plane. The properties of both materials were extracted from the materials database, using the standard ZnO and  $\text{Si}_{100}$  electrical and mechanical properties (see Tables S1 and S2, Supporting Information). The physics model was chosen to mimic the BC set up, clamping the Si side and applying the load on the ZnO face. To study the effect of the initial stress the resulting piezoelectric output the initial stress  $S_0$  was set as variable and modeled from 0 to  $1 \text{ N m}^{-2}$ . The constitutive piezoelectric equations considering initial stress are then as shown in Equations 1 and 2.

$$S = S_0 + s_E T + d^T E \quad (1)$$

$$D = d T + \epsilon_T E \quad (2)$$

where  $S$  is the strain,  $S_0$  is the initial stress,  $T$  is the stress,  $E$  is the electric field,  $D$  is the charge-density displacement,  $s$  is the elastic compliance matrix,  $d$  is the piezoelectric coefficient matrix and  $\epsilon$  is the material permittivity matrix. In the strain-charge form, relevant for BC measurements, the electric field is assumed to be constant or zero, therefore causing any change in the stress or strain of the material to be due to changes in the applied mechanical load.

### 2.6. Environmental Control

Subtle changes in temperature and humidity were compensated by the reference PZT in the system to maintain the set excitation. However, for thin film characterization, it might be considered if the difference in humidity was high as the higher adsorption of water molecules on the sample surface could create paths for the generated charges to dissipate therefore affecting the measurement, underestimating the actual  $d_{33}$  value. Therefore, the testing system was enclosed in a humidity chamber (Figure 1a), capable of monitoring both temperature and humidity using a commercial sensor (Govee H5075), tracking data throughout the study. Therefore, maintaining stable environmental conditions to ensure the minimal effect of temperature and humidity on both the reference PZT and the film under test. For the investigated studies, temperature and relative humidity were constantly monitored during the measurement. For all studies the environment was controlled and stable, showing values of  $21.2 \pm 0.1^\circ\text{C}$  and  $29.5 \pm 0.1\%$ , for both temperature and humidity, respectively.

## 3. Results and Discussion

### 3.1. Clamping Methods

Figure 3 presents the results of the piezoelectric coefficient measured during the first clamping of the sample and subsequent clamping (called here reclampings). For this study, two different methods, termed Method 1 (Figure 3a,b) and Method 2 (Figure 3c,d), were analyzed (see more details about both methods at Experimental Section). The time break between two subsequent reclaims corresponds to a 10 min break and each data point comprises the mean and standard variation of a 10-min long measurement. As Method 1 does not control accurately

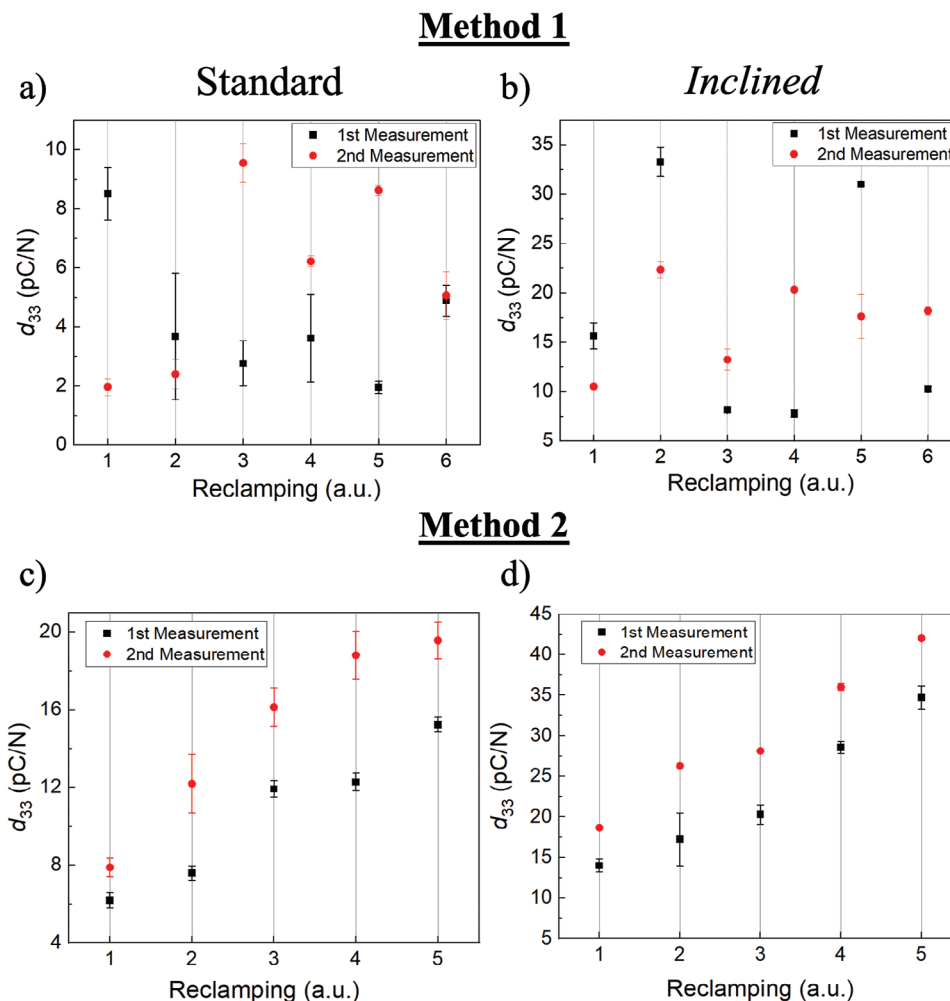


**Figure 3.** Piezoelectric coefficient versus reclamation using two methods. Method 1 a) standard and b) inclined ZnO thin films; Method 2 c) standard and d) inclined ZnO thin films. Each point corresponds to the average and standard deviation of a 10 min measurement. For each reclamation a 10 min break relaxation time (i.e., samples unloaded from the BC system) was inserted. Each measurement was repeated with a 24 h break to study the repeatability of the utilized method. Clamping and dynamic force were fixed to 1 N and  $0.4 N_{pp}$ , respectively; and frequency to 110 Hz. The data from which averages and standard deviation were extracted is available in Figures S1 and S2 (Supporting Information), for Method 1 and Method 2, respectively.

the loading of the sample on the system stage, it is observed in Figure 3a,b how the randomized clamping of the sample in the BC results in a chaotic distribution of results after each reclamation (Figure 3a,b). Moreover, measurements are non-consistent for each measurement within the sample when the reclamation is done with no control of the excited area. This result evidences the issues associated with use of this method on the determination of the true value of  $d_{33}$ , and specially for low  $d_{33}$  materials such as thin films. This drawback could be minor for the case of large piezoelectric coefficients, e.g., in PZT with  $d_{33}$  of hundreds of  $pC N^{-1}$ , however in the case of crystalline thin films of metal nitrides or metal oxides, showing  $d_{33}$  of tens of  $pC N^{-1}$ , Method 1 is unviable. For standard ZnO films, in Method 1, it is also observed the standard deviation is higher than the one shown by inclined films (Figure 3a,b). On possible explanation for that behavior is the existence of a diversity of excited piezoelectric domains within the lattice structure, resulting in a different  $d_{33}$  value every time the sample is measured, making the characterization of

thin films to be accompanied by errors that can underestimate or overestimate the piezoelectric output of the material, thereby invalidating, once more, Method 1 efficacy. Finally, to compare repeatability and robustness of the method, the measurement was repeated after 24 h. The results for Method 1 indicate the resulting piezoelectric coefficient does not follow a particular trend, but a chaotic distribution, demonstrating once again how Method 1 should be avoided for piezoelectric characterization.

In Figure 3c,d, it can be observed the resulting piezoelectric coefficient evolution as a function of the reclamation utilizing Method 2. In this case, for both standard and inclined ZnO thin films it is observed how the  $d_{33}$  increases for every reclamation. To ensure that the rising effect was not occurring due to systematic errors of the measurement, the study was repeated after 24 h, as done for Method 1, leaving the samples to relax and recover initial  $d_{33}$  values. The results are shown in the graph displayed in Figure 3c,d. The trend is observed again which confirms the pattern is a consequence of a material characteristic.

Now, if the stress is measured using an external technique (e.g., XRD, or capacitive stress measurements), calibration of the regression function presented in Figure 3c,d could be obtained, allowing the prediction/estimation of stress in samples with certain  $d_{33}$  or vice versa. Moreover, another important observation could be extracted from this Method 2. One could conclude that after 24 h the sample is not able to show the initial  $d_{33}$  values, exhibiting  $8.1 \text{ pC N}^{-1}$  (instead of  $6.4 \text{ pC N}^{-1}$ ) and  $18.2 \text{ pC N}^{-1}$  (instead of  $14.3 \text{ pC N}^{-1}$ ) for standard and inclined films, respectively. This observation suggests that after the initial measurement, the structure retains a “memory” of its previous state. This “memory”, in other words accumulated stress, prevents the piezoelectric domain from reverting back to its original state in the studied time frame of 24 h. To further investigate this effect, future studies could extend the “recovery time” to determine the minimum duration required for the piezoelectric material to alleviate the additional stress induced during measurements.

The observed increase of the piezoelectricity when the sample is excited over time can be explained by understanding the stress accumulation in the crystal structure when the film is exposed to constant excitation during several measurements. When a relaxed sample is being measured (in this work, a relaxed sample is considered that sample resting for at least 24 h), the piezoelectric domains are excited by an oscillating dynamic force ( $F_d$ ) that induces a mechanical strain in the lattice of the crystal and therefore creates an extrinsic effective stress in the material. When the sample is then removed and reclamped into the BC for the next measurement, the crystalline structure of ZnO films presents a residual stress which responds stronger to an external force stimulus generating more charge, therefore displaying a higher value of  $d_{33}$ . This accumulation of residual stress appears to be increasing the value of the output up to a limited number of measurements. To demonstrate the increase of the piezoelectric output of ZnO thin films is due to the accumulation of residual stress when characterizing them using BC, FEA was performed in COMSOL.<sup>[31]</sup> To the best of our knowledge, there is no report of the residual stress accumulation in crystals when characterizing piezoelectricity using BC, however, such effect has been observed for ceramics.<sup>[32]</sup> The study demonstrated the measured charge was larger than that estimated from stress-induced equations, indicating then the residual stress was influencing the output charge of the piezoelectric material. For the estimation of the “true value” of the piezoelectric coefficient  $d_{33}$ , it is considered here the first re-clamping of the series, ensuring that no internal stress is accumulated in the structure.

Due to the observed repeatability and robustness of the results obtained using Method 2, it is recommended that this protocol is used every time the BC technique is used to characterize piezoelectric thin film materials. Repeatability and robustness are here understood as the obtention of the observed trend when re-measuring after 24 h. That together with the results in the following section confirm the validity and improvement of using Method 2. This repeatability is not observed in Method 1 due to the different area of the sample that is excited each re-clamping, losing the control and the accuracy of the piezoelectricity measurement. As such Method, 2 was used for the rest of the studies in this work, including for the calculation of the “true value” of the  $d_{33}$ .

Comparing the piezoelectric coefficient values obtained for standard and inclined nanostructured thin films, one can con-

clude that inclined films exhibit a higher piezoelectric output ( $d_{33} = 14.3 \text{ pC N}^{-1}$ ) for the same measurement conditions that their counterpart standard film ( $d_{33} = 6.4 \text{ pC N}^{-1}$ ) in their original state (i.e., stress-free). This increase in the  $d_{33}$  coefficient of inclined films could be originated by the change in the anisotropy of the crystal typically observed in inclined nanostructured films deposited under OAD conditions.<sup>[33,34]</sup>

### 3.1.1. Simulation of $d_{33}$ Coefficient under Mechanical Stress

Figure 4a presents the 3D CAD model of a disc shape sample utilized here for the FEA. It can be observed that the ZnO thin film of  $1 \mu\text{m}$  is placed on top of a 0.5-mm thick Si piece with material properties described in Experimental Section. Figure 4b shows the estimated piezoelectric coefficient  $d_{33}$  (see Equation S1, Supporting Information) as a function of the initial material stress  $S_0$ . It is observed how the increase of the initial stress in the structure before the measurement can lead to an increase in the piezoelectric response, hence a higher resulting  $d_{33}$ . This corroborates the result obtained experimentally where the resulting piezoelectric coefficient increased after every measurement. It confirms the accumulation of the stress in the structure before launching a consecutive measurement affects the measured piezoelectric coefficient. In Figure 4c, it can be observed the gradual increase of the generated piezopotential consequence of an increase in the initial stress before the measurement. The picture corresponds to a cross-section snapshot of the geometry (Figure 4a), displaying the induced piezopotential under a distributed load of 1 N in the z-direction.

To extend further the results from the simulations, a linear fitting was obtained from the data in Figure 4b. Equation 3, relates then the  $d_{33}$  versus the initial stress of the sample  $S_0$  for the simulated geometry and selection of materials. This empirical expression assumes the material is a crystalline thin film of ZnO deposited on a crystalline substrate of Si, and exhibits a stress-free piezoelectric coefficient of  $6.4 \text{ pC N}^{-1}$ .

$$d_{33,S_0} = 6.4 + 6 S_0 \quad (3)$$

As suggested above, this equation could be used to predict  $d_{33}$  in different scenarios, where a piezometer is not available, measuring the relative stresses of the film with an external technique. Due to the linear dependency between  $d_{33}$  and  $S_0$ , we could obtain similar equation for our specific material. Knowing the intercept corresponds to the stress-free piezoelectric coefficient (i.e., first measurement after deposition) and the consecutive  $d_{33}$  measurements, it is possible to estimate the amount of residual stress induced by measuring in BC.

To understand the effect of residual stress accumulation it is possible to also use XRD characterization immediately after every BC measurement, however, due to sample transportation and manipulation between techniques the sample stress could be adversely influenced by several errors that could hinder the obtaining reliable data. Equation 4, based on the XRD peak shifts,<sup>[35–37]</sup> provides the expected peak shift for a given film stress deduced from Figure 4b.

$$(\Delta 2\theta) = 4 \frac{v_f}{E_f} \tan(2\theta_0) \sigma_f \quad (4)$$

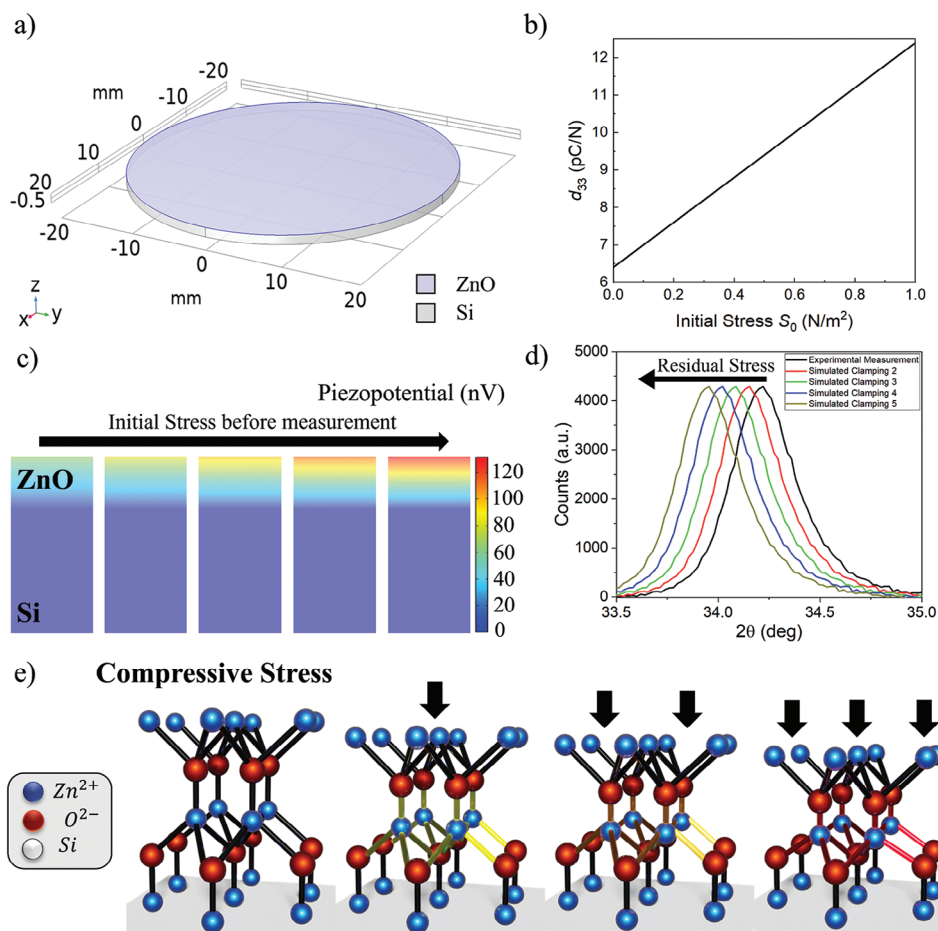


**Figure 4.** a) Geometry model used in simulations. b) FEA results of the  $d_{33}$  measurements as a function of the initial stress  $S_0$ . c) Generated piezopotential evolution as a function of increasing the initial stress before the measurement was carried. The graph displays snapshots taken at  $S_0 = 0, 0.25, 0.5, 0.75$  and  $1 \text{ N m}^{-2}$ . For the simulation,  $1 \text{ N m}^{-2}$  was applied as static load. d) XRD real and simulated peak shift (using Equation 4 and the stress data from simulations) due to residual stress. The four simulated peaks would correspond to the reclamping scenarios 2, 3, 4 and 5. e) 3D rendered image of the ZnO wurtzite structure under increasing compressive mechanical stress (from left to right).

where  $\Delta 2\theta$  corresponds to the XRD peak shift from the stress-free position  $\theta_0$  ( $34.42^\circ$ <sup>[38]</sup>),  $E_f$  represents the ZnO Young's Modulus ( $124 \text{ GPa}$ <sup>[36]</sup>),  $\nu_f$  is the Poisson's ratio ( $0.3$ <sup>[36]</sup>), and  $\sigma_f$  is the stress in the film.

Figure 4d shows the experimental XRD pattern of the standard ZnO measured as deposited, with the (0002) wurtzite peak centered at  $2\theta = 34.21^\circ$ , indicating there is an intrinsic compressive stress of  $-2.85 \text{ GPa}$  induced during the deposition process. Additionally, in Figure 4c, it can be observed the expected XRD peak simulated with the corresponding accumulated residual stresses after measuring in BC for the reclamplings 2 to 5. The shift is expected to be toward lower  $2\theta$  as the applied force during measurements is causing a compressive stress in the film, hence reducing the interplanar distance of the atoms, as predicted by Bragg's law (Equation 5).<sup>[39]</sup>

$$n\lambda = 2d_{\text{int}} \sin\theta \quad (5)$$

where  $n$  is an integer number, indicating constructive interference;  $\lambda$  corresponds to the wavelength of the XRD measurement,

$d_{\text{int}}$  represents the interplanar distance and  $\theta$  is the angle of incidence of the x-ray.

XRD diffractogram showed in Figure 4d corresponds to (002) diffraction peak of ZnO crystal. ZnO presents a wurtzite structure consisting of a hexagonal close-packed array of oxygen anions with half of the tetrahedral voids occupied by zinc cations (see Figure 4e). As suggested by Figure 3 and simulations of Figure 4c, applying a mechanical stress to the ZnO lattice, results in electric dipoles with higher intensity than those observed in absence of an initial stress. As represented with a colour gradient in the bonds of the atoms of the ZnO structure (Figure 4e), the greater the initial stress applied to the structure, the higher the value of the electric dipole.

### 3.2. Study of $d_{33}$ Versus Time and Actuation Frequency

Figure 5a,b shows the BC measurements carried out in standard and inclined ZnO thin films, respectively. From those graphs, it can be observed that  $d_{33}$  coefficient varies over time. At the be-



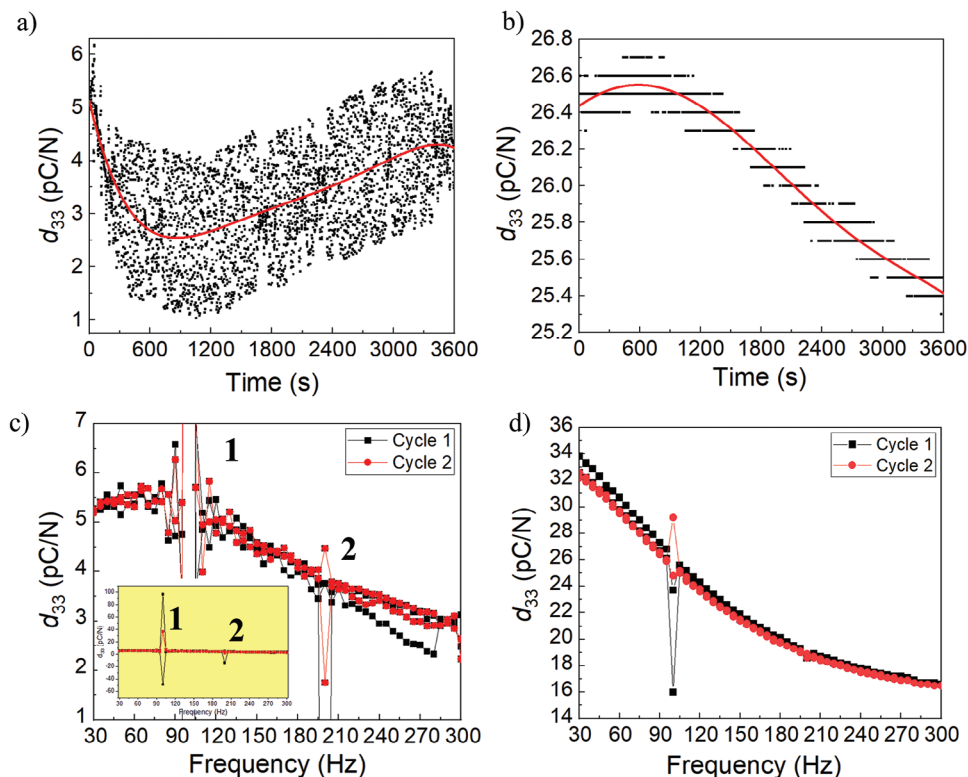


**Figure 5.** Piezoelectric coefficient versus time for a) standard and b) inclined ZnO thin films. The measurement ran for 1 h in total. Resolution of the system changes from 0.1 to 0.01 pC N<sup>-1</sup> when measuring  $d_{33}$  values below 10 pC N<sup>-1</sup>, hence the difference in the resulting noise difference. Red line represents the average value for easier visualization. The static and dynamic force utilized for the study were set to 1 N and 0.25 N<sub>pp</sub>, respectively. Frequency of 110 Hz. Piezoelectric coefficient versus frequency for c) standard and d) inclined ZnO thin films. The study measured the  $d_{33}$  from 30 to 300 Hz for two full cycles to observe possible hysteretic behaviors. Main power resonance peaks are numbered 1 and 2 at frequencies 100 and 200 Hz. The rest of the parameters were fixed, static force being 1 N and dynamic force being 0.25 N<sub>pp</sub>. Each point comprises an average of a 1 min of data at the beginning of the measurement.

ginning of the measurement, standard films exhibit  $d_{33}$  values  $\approx 5$  pC N<sup>-1</sup>, dropping to 2.5 pC N<sup>-1</sup> after 600 s of analysis (↓50% of its initial value), and increasing to values  $\approx 4$  pC N<sup>-1</sup> for times  $\approx 1$  h (↓20% of its initial value). In contrast, inclined films showed a different variation of the piezoelectric coefficient, exhibiting an increase from 26.4 to 26.6 pC N<sup>-1</sup> for a time window of 600 s (↑0.6% of its initial value), and a drop of the value down to 25.4 pC N<sup>-1</sup> after 1 h (↓4% of its initial value). From this time study, it is possible to extract various conclusions: i) inclined films present higher  $d_{33}$  than standard films, being in good agreement with the literature<sup>[14]</sup>; ii)  $d_{33}$  of inclined and standard films show different time dependency, the former slightly increases up to a point where starts its decay, and the latter exhibiting a decay and an increase; iii)  $d_{33}$  of thin films varies over time, which is in good agreement with previous works reported in the literature but for ceramic materials<sup>[14]</sup>; iv) the variation of the  $d_{33}$  coefficient measured in inclined films shows a more stable response over time compare to those obtained in standard films.

The variation of  $d_{33}$  over time observed in ceramic materials is reported to follow a decreasing and saturation curve from the starting time onward.<sup>[14]</sup> The time where the measurement reaches saturation region is concluded to be material dependent and no definite explanation is given, however it is suggested for thinner ceramics that several mechanisms are affecting the stress

relaxation inside the material. Another difference between ceramics and our ZnO thin films is observed. Whereas for ceramics the steepest change occurs in the first 100s, for our crystalline thin films is observed to be extended for the first 600s, and subsequently the system extended for the first 600s, after that time, the system follows increase or decrease for standard or inclined films, respectively, until saturation occurs. Temperature, humidity, and mechanical stress, as well as electric field amplitude and frequency used during the BC characterization, are the main parameters affecting the  $d_{33}$  coefficient of a piezoelectric material. In our study, since the temperature and humidity are constant, as well as the input mechanical stimulus (amplitude and frequency of the dynamic and static forces), the only magnitude that could vary as effect of the time is the accumulation of the mechanical stress in the ZnO crystalline structure.

Figure 5c,d shows the frequency hysteresis result for standard and inclined ZnO thin films, respectively. The operation frequencies of BC range from 30 to 300 Hz ensuring the measurement is performed far from any material resonant frequency, which would lie on the kHz region as demonstrated by FEA simulations (not shown). In ceramics the expected  $d_{33}$  behavior on the range of frequencies is to increase as frequency increased due to the system approaching a resonant frequency,<sup>[14]</sup> for piezoelectric thin films this effect is not observed as resonant frequencies

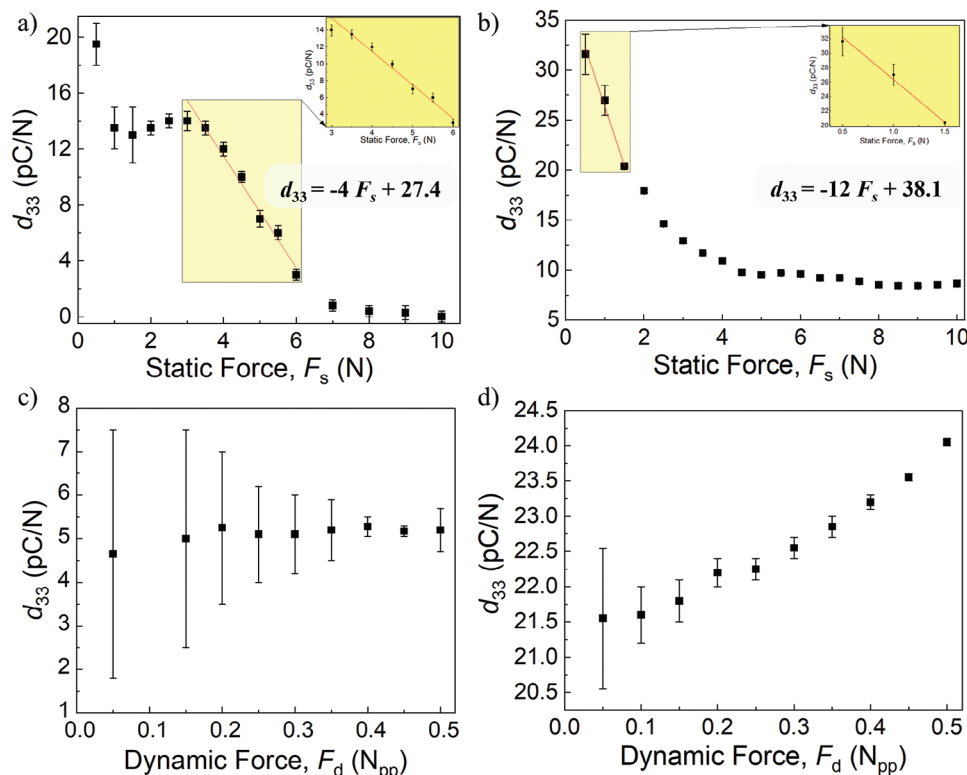


**Figure 6.** Piezoelectric coefficient versus static force for a) standard and b) inclined ZnO thin films. Insets represent the linear fitting for the linear response section of the  $d_{33}$  with the static force. The calculated sensitivity for both samples is estimated to be  $\approx 4$  and  $\approx 12$  pC N<sup>-2</sup>, respectively. Piezoelectric coefficient versus dynamic force for c) standard and d) inclined ZnO thin films, the static force is fixed at 2 N for both samples. The frequency of all the measurements in the figure is fixed to 110 Hz and every measurement consists of an averaging of 10 min of piezoelectric data for each step in both static and dynamic force.

are far removed from the measurement range due to their reduced thickness. The measured  $d_{33}$  in our thin films is observed to decrease when increasing the frequency for both standard and inclined films. The same percentage of change is observed for both films ( $\approx 50\%$ ). Due to being far from any resonant frequency of the material, the increase in frequency produces a decrease in the piezoelectric output caused by a reduced domain mobility the structure suffers, this has also been reported for soft piezoelectric ceramics.<sup>[14]</sup> It is worth mentioning how there could be observed an anomaly  $\approx 100$  and 200 Hz (Figure 5c,d inset). This is related to the main power frequency (50 Hz in the UK) and two corresponding harmonic frequencies, a consequence of a non-perfect system isolation from the building electric grid. Finally, Figure 5c,d also proves that both films do not present any hysteresis, which demonstrates the potential of the sputtered films for their utilization as piezoelectric components in applications described above.

### 3.3. Effects of Static and Dynamic Force on $d_{33}$ Coefficient

The effect of static ( $F_s$ ) and dynamic ( $F_d$ ) forces on the measured  $d_{33}$  was investigated. **Figure 6a,b** shows the  $d_{33}$  evolution whilst increasing  $F_s$  for standard and inclined thin films, respectively. From these figures, there are two main conclusions. First, the reduction of the error bars as  $F_s$  increases; indicating that exper-

imental method is more reliable for higher  $F_s$ , as this condition keeps the sample position stable, and makes the process more repeatable from measurement-to-measurement. Second, for low  $F_s$  ( $<1$ N) the sample rattles because of the clamping not being enough, therefore an extra stress is accounted from vibrational motions generating additional charge that overestimate the  $d_{33}$ . For the sake of completion, the effect of these external vibrations will be analyzed later. For standard ZnO thin films, there exists a stable region ranged between 1 and 3N where the measurement is constant. To the best of our knowledge, this is the first report highlighting the importance of choosing that *plateau* in similar piezometers based in BC to improve the systematic uncertainty of the system. For higher pre-loads ( $F_s > 3$ N), and as seen for soft ceramics<sup>[14]</sup> the excessive increase of  $F_s$  causes a drastic decrease in the measured  $d_{33}$  due to the large applied force that limits the mobility of the piezoelectric upon induced deformation (i.e., mechanical strain). This scenario is even more evident when  $F_s > 6$ N are utilized, exhibiting a  $d_{33}$  of zero (Figure 6a). For inclined films a similar behavior is observed for low forces, i.e.,  $d_{33}$  decreases from 33 down to 10 pC N<sup>-1</sup>, as  $F_s$  increases from 0.5 to 4 N. Inclined films do not show a stable region until  $F_s$  reaches 4N. Then, the measured  $d_{33}$  is capped to  $\approx 8$ pC N<sup>-1</sup>. Inclined films do not show a null  $d_{33}$  value for the whole range of  $F_s$  under investigation. However, it is worth noting that high forces are again limiting the domain mobility, and thus, underestimating the piezoelectric output. From the application point of view,

inclined films might be used at a higher  $F_s$  compared to those tolerated by standard films, however, the performance of these films will not be at full potential as clearly observed in Figure 6b. If piezoelectric films are proposed to be used as sensing material, then, the area of interest will be that showing  $d_{33}$  variation with  $F_s$ . Insets in Figure 6a,b, shows a fitting of the linear region of the graph, resulting in a sensitivity of the standard and inclined film of  $4 \pm 0.3$  and  $12 \pm 1$  pC N<sup>-2</sup> (corresponding to the change of pC N<sup>-1</sup> per N of applied force), respectively. From those results, one could conclude that both films could play an excellent role as active layers in pressure sensors, however, inclined films would present a higher resolution in sensing forces due to the enhanced sensitivity. For example, they could be used in tactile skin applications, where monitoring of the pressure could provide feedback information.<sup>[40–42]</sup>

Figure 6c,d shows the effect of the dynamic force on the measurement of  $d_{33}$ . For standard ZnO films, it is observed how the average value is constant for the whole range of  $F_d$ , however it is noted an increase of the signal-to-noise ratio (SNR) when increasing  $F_d$ . Despite this SNR, Figure 6c clearly shows that  $d_{33}$  does not change with  $F_d$  in standard films. From those results, one could recommend carrying out the measurements at higher  $F_d$  to prevent effects of SNR. In contrast, for inclined films, the  $d_{33}$  increases with  $F_d$ . This distinct behavior can be attributed to the difference in the microstructure of an inclined film compared to a standard sample. Inclined films exhibit by their nature a less dense structure that allows higher domain mobility when higher forces are applied, therefore generating more charges that account for the piezoelectric output.

#### 4. Conclusion

This work presents a comprehensive revision of the quasi-static method conventionally utilized to measure the  $d_{33}$  coefficient in thick piezoelectric materials (typically ceramics), to make it compatible with the characterization of piezoelectric thin films. The method improvements comprised the implementation of a Python code for the data acquisition, and a new self-centering adapter in a commercial BC system, the latter ensuring a soft-applied force, reliable, stable, and repeatable measurement of the  $d_{33}$  over time. The new adaptor allowed to carry out measurements of  $d_{33}$  as a function of excitation frequency (hysteresis analysis), static and dynamic forces, whilst monitoring temperature and humidity.

Standard and inclined nanostructured ZnO thin films were analyzed by the optimized process with the aim of pushing the improved technique to its limits. From the two methods tested, Method 2 is here proposed as crucial to obtain a repeatable valid piezoelectric coefficient in thin film characterization. The results of the FEA simulations suggest that the accumulation of residual stress in the structure is the reason why the piezoelectric output observed on the experimental BC measurements increases after few measurements. From the experiment, it is observed 24 h is not enough time for the structure to alleviate the accumulated stress and recover the original  $d_{33}$  value. The time results indicate the material presents a “warm-up” period to reach stable readings. This information could impact the way these films are used for sensing applications, as it gives indication of a “warm-up period” the structure requires to function at a stable performance.

Also, it is demonstrated how inclined films show a lower relative variation (4% from initial value), important for their use in actuation or sensing applications, whereas standard films change 20–50% for the same measurement time, hindering their use in real applications. From frequency studies, it has been observed no hysteretic behavior and a reduction of piezoelectric output when increasing frequency for both studied films. Force studies allowed the optimization of the parameters to optimize the stability of the measurement and increase the SNR. Also provided information of the force sensitivity ( $\approx 4$  and  $\approx 12$  pC N<sup>-2</sup>) both films offer for their use, for example, as pressure sensors. All in all, differences between standard and inclined ZnO films have been observed for most of the studies, reinforcing the need to optimize the Berlincourt method for the specific material under test.

#### Supporting Information

Supporting Information is available from the Wiley Online Library or from the author.

#### Acknowledgements

This research is partially supported by CENSIS, Novosound Ltd., University of the West of Scotland and the Institute of Thin Films, Sensors, and Imaging (ITFSI).

#### Conflict of Interest

The authors declare no conflict of interest.

#### Data Availability Statement

The data that support the findings of this study are available from the corresponding author upon reasonable request.

#### Keywords

Berlincourt, piezoelectric materials, quasi-static method, thin films, zinc oxide

Received: August 13, 2023

Revised: October 24, 2023

Published online:

- [1] Y. Wu, Y. Ma, H. Zheng, S. Ramakrishna, *Mater. Des.* **2021**, *211*, 110164.
- [2] J. F. Tressler, S. Alkoy, R. E. Newnham, *J. Electroceram.* **1998**, *2*, 257.
- [3] X. Gao, J. Yang, J. Wu, X. Xin, Z. Li, X. Yuan, X. Shen, S. Dong, *Adv. Mater. Technol.* **2020**, *5*, 1900716.
- [4] M. Stoppa, A. Chiolerio, *Sensors* **2014**, *14*, 11957.
- [5] Q. Zhou, S. Lau, D. Wu, K. Kirk Shung, *Prog. Mater. Sci.* **2011**, *56*, 139.
- [6] X. S. Zhou, C. Zhao, R. Hou, J. Zhang, K. J. Kirk, D. Hutson, Y. J. Guo, P. A. Hu, S. M. Peng, X. T. Zu, Y. Q. Fu, *Ultrasonics* **2014**, *54*, 1991.
- [7] J.-F. Li, *Lead-Free Piezoelectric Materials*, Wiley-VCH, Weinheim, Germany **2021**.
- [8] X. B. Wang, C. Song, D. M. Li, K. W. Geng, F. Zeng, F. Pan, *Appl. Surf. Sci.* **2006**, *253*, 1639.

- [9] C. Thring, F. Band, D. Irving, K. McAughey, D. A. Hughes, in IEEE Int. Ultrasonics Symp. (IUS), IEEE, Piscataway, NJ **2020**.
- [10] Y. Li, K.-S. Moon, C. P. Wong, *Science* **2005**, 308, 1419.
- [11] P. K. Panda, B. Sahoo, *Ferroelectrics* **2015**, 474, 128.
- [12] H. Wei, H. Wang, Y. Xia, D. Cui, Y. Shi, M. Dong, C. Liu, T. Ding, J. Zhang, Y. Ma, N. Wang, Z. Wang, Y. Sun, R. Wei, Z. Guo, *J. Mater. Chem. C Mater.* **2018**, 6, 12446.
- [13] C. Campbell, *Surface Acoustic Wave Devices and their Signal Processing Applications*, Elsevier, Amsterdam, Netherlands **1989**.
- [14] M. G. Cain, *Characterisation of Ferroelectric Bulk Materials and Thin Films*, Dielectric Breakdown in Dielectrics and Ferroelectric Ceramics, Vol. 2, Springer, Berlin, Germany **2014**.
- [15] S. Trolier-Mckinstry, P. Muralt, *J. Electroceram.* **2004**, 12, 7.
- [16] D. Hu, M. Yao, Y. Fan, C. Ma, M. Fan, M. Liu, *Nano Energy* **2019**, 55, 288.
- [17] I. Kanno, H. Kotera, K. Wasa, *Sens. Actuator A Phys.* **2003**, 107, 68.
- [18] R. Herdier, D. Jenkins, E. Dogheche, D. Rèmesiens, M. Sulc, *Rev. Sci. Instrum.* **2006**, 77, 093905.
- [19] Y. Calahorra, X. Guan, N. N. Halder, M. Smith, S. Cohen, D. Ritter, J. Penuelas, S. Kar-Narayan, *Semicond. Sci. Technol.* **2017**, 32, 074006.
- [20] S. Sriram, M. Bhaskaran, K. T. Short, G. I. Matthews, A. S. Holland, *Micron* **2009**, 40, 109.
- [21] A. Gomez, M. Gich, A. Carretero-Genevri, T. Puig, X. Obradors, *Nat. Commun.* **2017**, 8, 1113.
- [22] R. Pérez, N. Chaillet, K. Domanski, P. Janus, P. Grabiec, *Sens. Actuator A Phys.* **2006**, 128, 367.
- [23] Z. Huang, Q. Zhang, S. Corkovic, R. Dorey, R. Whatmore, *IEEE Trans. Sonics Ultrason.* **2006**, 53, 2287.
- [24] F. Xu, F. Chu, S. Trolier-Mckinstry, *J. Appl. Phys.* **1999**, 86, 588.
- [25] M.-A. Dubois, P. Muralt, *Sens. Actuator A Phys.* **1999**, 77, 106.
- [26] J. E. A. Southin, S. A. Wilson, D. Schmitt, R. W. Whatmore, *J. Phys. D Appl. Phys.* **2001**, 34, 1456.
- [27] J. F. Shepard, P. J. Moses, S. Trolier-Mckinstry, *Sens. Actuator A Phys.* **1998**, 71, 133.
- [28] D. Berlincourt, H. Jaffe, *Phys. Rev.* **1958**, 111, 143.
- [29] M. Pelayo Garcia, K. L. McAughey, D. Gibson, D. A. Hughes, C. Garcia Nuñez, In *2021 13th Spanish Conf. on Electron Devices (CDE)*, IEEE, Piscataway, NJ **2021**.
- [30] C. T. Rueden, J. Schindelin, M. C. Hiner, B. E. DeZonia, A. E. Walter, E. T. Arena, K. W. Eliceiri, *BMC Bioinform.* **2017**, 18, 529.
- [31] COMSOL Multiphysics®, COMSOL AB, Stockholm, Sweden.
- [32] F. Xu, PhD thesis, The Pennsylvania State University, **1999**.
- [33] S. Bairagi, K. Järrendahl, F. Eriksson, L. Hultman, J. Birch, C.-L. Hsiao, *Coatings* **2020**, 10, 768.
- [34] A. Barranco, A. Borrás, A. R. Gonzalez-Eliphe, A. Palmero, *Prog. Mater. Sci.* **2016**, 76, 59.
- [35] M. Dailey, Y. Li, A. D. Printz, *ACS Omega* **2021**, 6, 30214.
- [36] H. F. Pang, Y. Q. Fu, R. Hou, K. J. Kirk, D. Hutson, X. T. Zu, F. Placido, *Ultrasonics* **2013**, 53, 1264.
- [37] B. D. Cullity, S. R. Stock, *Elements of X-Ray Diffraction*, Addison-Wesley, Boston, **1956**.
- [38] V. Polewczyk, R. Magrin Maffei, G. Vinai, M. Lo Cicero, S. Prato, P. Capaldo, S. Dal Zilio, A. Di Bona, G. Paolicelli, A. Mescola, S. D'addato, P. Torelli, S. Benedetti, *Sensors* **2021**, 21, 6114.
- [39] W. H. Bragg, W. L. Bragg, *Proc. R. Soc. Lond. A* **1913**, 88, 428.
- [40] L. Zou, C. Ge, Z. Wang, E. Cretu, X. Li, *Sensors* **2017**, 17, 2653.
- [41] M. I. Tiwana, S. J. Redmond, N. H. Lovell, *Sens. Actuator A Phys.* **2012**, 179, 17.
- [42] C. García Núñez, L. Manjakkal, R. Dahiya, *npj Flexible Electron.* **2019**, 3, 1.